

Supernova neutrinos and nucleosynthesis

G. Martínez-Pinedo^{1,2}, T. Fischer³, L. Huther¹

¹Institut für Kernphysik (Theoriezentrum), Technische Universität Darmstadt, Schlossgartenstraße 2, 64289 Darmstadt, Germany

²GSI Helmholtzzentrum für Schwerionenforschung, Planckstraße 1, 64291 Darmstadt, Germany

³Institute for Theoretical Physics, University of Wrocław, pl. M. Borna 9, 50-204 Wrocław, Poland

E-mail: gabriel.martinez@physik.tu-darmstadt.de

Abstract. Observations of metal-poor stars indicate that at least two different nucleosynthesis sites contribute to the production of r-process elements. One site is responsible for the production of light r-process elements $Z \lesssim 50$ while the other produces the heavy r-process elements. We have analyzed recent observations of metal-poor stars selecting only stars that are enriched in light r-process elements and poor in heavy r-process elements. We find a strong correlation between the observed abundances of the $N = 50$ elements (Sr, Y and Zr) and Fe. It suggests that neutrino-driven winds from core-collapse supernova are the main site for the production of these elements. We explore this possibility by performing nucleosynthesis calculations based on long term Boltzmann neutrino transport simulations. They are based on an Equation of State that reproduces recent constraints on the nuclear symmetry energy. We predict that the early ejecta is neutron-rich with $Y_e \sim 0.48$, it becomes proton rich around 4 s and reaches $Y_e = 0.586$ at 9 s when our simulation stops. The nucleosynthesis in this model produces elements between Zn and Mo, including ^{92}Mo . The elemental abundances are consistent with the observations of the metal-poor star HD 12263. For the elements between Ge and Mo, we produce mainly the neutron-deficient isotopes. This prediction can be confirmed by observations of isotopic abundances in metal-poor stars. No elements heavier than Mo ($Z = 42$) and no heavy r-process elements are produced in our calculations.

Submitted to: *J. Phys. G: Nucl. Part. Phys.*

1. Introduction

Core-collapse supernova occur at the end of the evolution of massive stars when the core collapses to form a proto neutron star (PNS) [1, 2]. The energy gain during the collapse corresponds to the gravitational binding energy of the PNS, $\approx 3 \times 10^{53}$ ergs, and is emitted as neutrino radiation on time scales of tens of seconds during which the central PNS cools, deleptonizes and contracts to the final neutron star. This corresponds to an emission of 10^{58} (anti)neutrinos of all flavors with typical energies of 10–15 MeV. Given the large amount of neutrinos involved, it is expected that they will play an important role in both the supernova dynamics and the underlying nucleosynthesis.

At present, the delayed neutrino-heating mechanism [3] represents the most promising scenario to explain supernova explosions. In fact, recent two-dimensional simulations [4, 5, 6] produce neutrino driven explosions on time scales of several hundreds of milliseconds after bounce. Once the explosion sets in, the continuous emission of neutrinos from the PNS drives a low-mass outflow known as neutrino-driven wind [7] that is currently considered a favored site for the productions of elements heavier than iron (e.g. [8]). As neutrinos travel through the stellar mantle, they can suffer flavor oscillations [9, 10], contribute to the nucleosynthesis of several rare isotopes [11, 12] and even drive an r process in the He-shell of metal-poor stars [13] before they are finally detected on Earth.

This paper addresses several issues related to the role of neutrinos on the nucleosynthesis of heavy elements in core-collapse supernova explosions. After discussing recent constraints from metal-poor stars observations on the production of heavy elements by the r-process (section 2), we describe different nuclear physics aspects that are relevant to determine the luminosities and spectra of neutrinos emitted during the PNS deleptonization which proceeds via weak processes. For those involving nucleons (section 3), corrections due to the nuclear interaction are relevant due to the relatively high density in the decoupling region. They are particularly important for charged-current processes and are related to the symmetry energy of nuclear matter. New long term Boltzmann transport simulations of the neutrino-driven wind are presented in section 4 and its nucleosynthesis yield discussed.

2. Implications from metal-poor star observations

Traditionally the production of elements heavier than iron has been associated with two neutron capture processes, the r-process and the s-process [14, 15] with a smaller contribution due to the p-process (or γ -process) [16]. In this picture, the abundances of heavy elements observed in our Sun are the superposition of different events producing s-process elements (intermediate-mass AGB stars and massive stars) [17, 18, 19] and r-process elements in a so far not yet identified site(s) [20]. The so-called solar system r-process abundance is obtained by subtracting from the solar system isotopic abundances [21, 22, 23] the solar s-process pattern determined from a combination of

experimentally determined (n, γ) cross sections and AGB stellar models [24, 25].

Due to the long evolutionary time scales of intermediate mass stars before reaching the AGB phase (up to a billion years), it is expected that stars that are sufficiently old will have been enriched by the r-process but not by the s-process. (Provided that the r-process operates in a site with a much shorter evolutionary time scale than the s-process sites). Astronomers use the metallicity, normally associated with the abundance of Iron in the star, as a proxy for the age. Metal-poor stars, $[\text{Fe}/\text{H}] \lesssim -1.5\ddagger$, present abundances of heavy elements that do not correspond with the solar system s-process abundances [26, 27]. These stars, also called r-II stars [28], present robust abundance patterns that match almost perfectly the solar system r-process abundance pattern for elements with $Z > 50$ [26, 27, 29]. Some other stars [30, 31] are depleted in elements heavier than $Z = 50$ but enriched in lighter elements with $A \sim 90$ like Sr, Y and Zr. As these elements are abundantly produced in alpha-rich freeze-outs from neutrino-driven winds [32, 33] (see also section 4) by charged-particle reactions (CPR) they are sometimes denoted CPR elements [34]. This reference suggested a simple “LEGO-block” model to explain these observations. In this model the production of CPR (also known as light r-process) elements with $Z \lesssim 50$ and heavy r-process elements with $Z > 50$ is due to two different sources: 1) an H-source produces the heavy r-process elements together with CPR elements and no Iron with an abundance pattern as given by r-II stars; 2) an L-source produces light r-process elements or CRP elements with an abundance pattern given by the observations of HD 122563 [30, 31] together with Iron. In this model the H-source is the site where the “main” r-process operates while the L-source produces light r-process elements in what sometimes is denoted as “weak” r-process. Similar results were obtained in the Galactic chemical evolution study of ref. [35] that suggested the existence of a “lighter element primary process” (LEPP) to explain the abundances of Sr, Y and Zr at low metallicities. Here “process” has to be interpreted as a different astrophysical site to the one in which the “main” r-process operates (in this case the LEPP is analogous to the L-source of ref. [34]).

The above model explains the large scatter in the abundance of Eu observed at low metallicities [40, 27] (see upper left panel of figure 1). At early times the Galaxy is chemically unmixed and Eu is mainly produced in rare events with little or no iron production [41]. This model predicts that there may be stars that are only enriched in light r-process elements but so far all metal-poor stars observed contain both light and heavy r-process elements [42]. It may indicate that the relative low abundances of heavy r-process elements observed in stars that show an abundance pattern like HD 122563 are in fact produced together with light r-process elements but with much lower efficiency. If the L-source site is neutrino-driven winds from core-collapse supernova as suggested by ref. [34] it implies that neutrino-driven winds should produce also elements with $Z > 50$. In principle, there could be a large variability in the production of light r-process elements from event to event, however the work of ref. [43] suggest that their

\ddagger Astronomers use the $[A/B]$ notation to describe the relative abundances of two elements in a star compared to that in the Sun: $[A/B] = \log_{10}(N_A/N_B)_* - \log_{10}(N_A/N_B)_\odot$

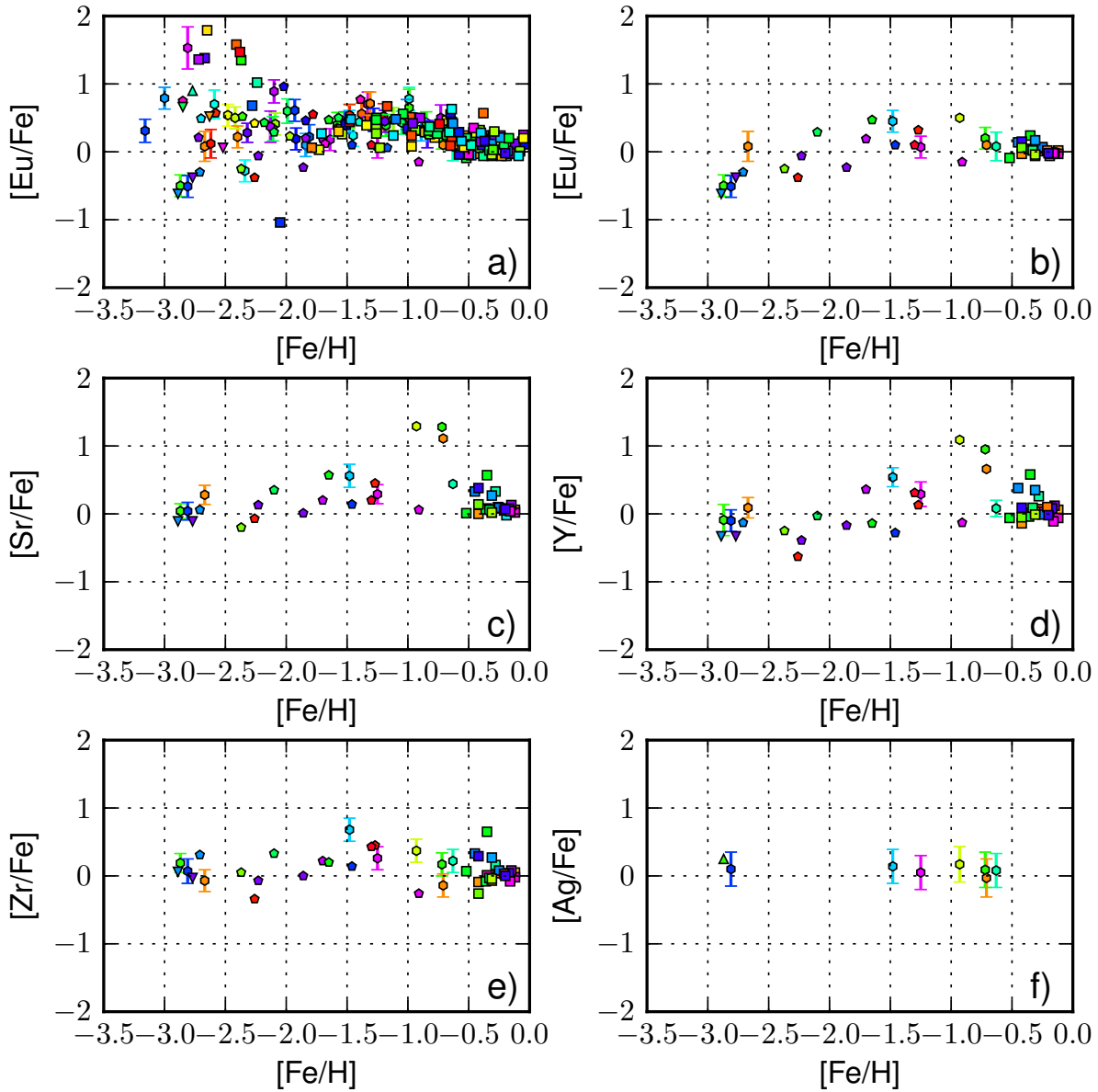


Figure 1. Abundance ratio of metal-poor stars [36, 37, 38, 39] as a function of metallicity, $[\text{Fe}/\text{H}]$. The upper left panel includes all metal-poor stars in the sample while all other panels include only stars whose abundance pattern can be related to an L-source event. They are enriched in light r-process elements and poor in heavy r-process elements.

production is robust and always results in an abundance pattern similar to the one observed in HD 122563.

If Eu ($Z = 63$) is in fact produced together with Fe in L-source events a plot showing stars that have been enriched by these events should show a correlation, i.e. $[\text{Eu}/\text{Fe}]$ should be constant as a function of metallicity. A star whose abundance pattern is due to an H-source event has a ratio Eu/Sr that is much larger than the one found in the solar system. Typical values are $[\text{Eu}/\text{Sr}] \sim 1$. Hence, we characterize stars polluted by an L-source event, i.e. enriched in light r-process elements, as those with $[\text{Eu}/\text{Sr}] < 0$.

A lower value could also be used but in this case the number of stars in the sample is largely reduced. This condition includes also stars that have been enriched mainly by the s-process but they should not be present at low metallicities. Figure 1 shows the [Eu/Fe], [Sr/Fe], [Y/Fe], [Zr/Fe], and [Ag/Fe] for a sample of metal-poor stars from recent compilations [36, 37, 38, 39]. Only stars with [Eu/Sr] < 0 are shown. It is intriguing to see that a correlation in [Eu/Fe] versus metallicity emerges that is absent once the whole sample of metal-poor stars is considered. This may suggest that Eu is co-produced together with Fe in the events that produce light r-process elements. A correlation is also found in Sr, Y and Zr that is expected if these elements are produced in neutrino-driven winds [34]. The scatter is also greatly reduced when compared to a sample without any selection criteria (see figures in refs. [35, 39]). The situation is unclear for Ag as only two stars have survived our criteria. A larger sample of metal-poor stars is required to check this hypothesis. Ref. [39] has found an anticorrelation between Ag and Pd and Sr, Y and Zr suggesting that both element groups are produced in different sites.

In the above discussion, we have explicitly avoided to mention possible sites for r-process nucleosynthesis. Several sites have been suggested for both the H-source and L-source events. It is likely that the production of both light and heavy r-process elements is dominated by different sites as a function of metallicity. Neutron star mergers are a likely site for H-source events. Recent simulations [44, 45] show that the material ejected dynamically during the merger is an ideal site for a robust r-process that produces nuclei with $A \gtrsim 120$ ($Z \gtrsim 50$) in agreement with the solar r-process abundance distribution [44, 45]. In this scenario, the production of nuclei with $A \sim 120$ is due to the fission of nuclei in the region of $A \sim 280$ and sensitive to the particular fission rates and yields used [46, 47]. Fission cycling is also responsible for producing a robust r-process pattern. An important aspect of r-process in neutron star mergers is that the amount of r-process material ejected is large enough ($10^{-3} M_{\odot}$ to $10^{-2} M_{\odot}$) to produce an optical/near-infrared transient powered by the radioactive decay of r-process nuclei [48, 49, 45]. The transient luminosity is expected to reach a maximum of $\sim 10^{42}$ erg s $^{-1}$, i.e. kilonova luminosities, in timescales of hours to days [48, 49, 45]. The observation of a near-infrared transient associated with the short γ -ray burst GRB130603B has been related to a kilonova type event powered by the decay of r-process nuclei [50, 51] (however see the caveats mentioned in ref. [52]). If confirmed, this will be the first direct observation of an r-process nucleosynthesis event and will demonstrate that neutron-star mergers are an r-process site. Neutron-star mergers are also expected to eject material from outflows from the accretion disk formed around the black hole remnant. This material will be ejected either by neutrino-driven winds [53, 52] or by viscous heating and recombination of nucleons into alpha particles [54]. These ejecta are expected to produce light r-process elements making neutron-star mergers a possible candidate to account for observations of r-II metal-poor stars. However, due to the long evolutionary timescales involved, neutron-star mergers have problems to explain for the r-process at low metallicities [55, 56]. Several sites

have been suggested that are expected to operate mainly at low metallicities: Jets from magnetorotational supernova [57] and a neutrino-induced r-process in the He shell of core-collapse supernova [13]. These sites produce mainly nuclei with $A \gtrsim 130$ but an additional contribution producing light r-process elements from neutrino-driven winds from the protoneutron star or black-hole accretion disk is expected.

Neutrino-driven winds from protoneutron stars have been suggested as the site for L-source events [34], i.e. light r-process elements. This aspect is analyzed in section 4 based on Boltzmann neutrino transport simulations.

3. Charged-current neutrino interactions in core-collapse supernovae

Neutrino-driven winds from protoneutron stars have been considered for a long time like a possible site for the nucleosynthesis of heavy elements (see ref. [8] for a recent review). It is expected that independently of the explosion mechanism a protoneutron star (PNS) will form after a core-collapse supernova explosion. The PNS deleptonizes by continuous emission of neutrinos of all flavors in a period of several tens of seconds. Neutrino absorption processes at the PNS surface deposit heat which drives a matter outflow known as the neutrino-driven wind [7]. Initial studies showed that neutrino-driven winds could be the site for the r-process [58, 59]. These pioneering works were followed by analytic [60], parametric [61] and steady state wind models [62, 63] that showed that neutrino-driven winds produce both light and heavy r-process elements provided that the outflow has short dynamical time scales (a few milliseconds), high entropies (above 150 k /nucleon) and low electron fractions ($Y_e < 0.5$). Recent hydrodynamical simulations [64, 65] show that the short dynamical timescales can in fact be achieved but fail however to obtain the necessary entropies at times relevant for r-process nucleosynthesis [66]. These works rule out the possibility that neutrino-driven winds are responsible for the production of heavy r-process elements with $Z \gtrsim 50$. In the following, we analyze the possibility that light r-process elements ($Z \gtrsim 50$) may be produced in neutrino winds.

The nucleosynthesis outcome of neutrino-driven winds is very sensitive to the electron fraction, Y_e , of the ejected matter [67, 68] that is determined by the competition between electron neutrino absorption in neutrons and antineutrino absorption in neutrons and their inverse reactions. These rates are rather sensitive to the luminosity and spectral differences between electron neutrinos and antineutrinos. The work of ref. [68] has shown that light r-process elements can be produced both in proton-rich and neutron-rich ejecta. However, the assumed Y_e evolutions need to be reevaluated on the light of recent works [69, 70, 71]. This aspect has recently been revisited in ref. [72].

Deep in the interior of the protoneutron star neutrinos are in thermal and chemical equilibrium with matter. However, as we move to the surface and the temperature and density drop neutrinos decouple with matter. As μ and τ neutrinos interact only via neutral current they are the first to decouple. For the very neutron rich conditions found at the PNS surface, electron antineutrinos decouple before electron neutrinos. As the

neutrino spectrum reflects the local properties of matter at the position in which they decouple, one expects the following hierarchy of neutrino energies: $\varepsilon_{\nu_{\mu,\tau}} > \varepsilon_{\bar{\nu}_e} > \varepsilon_{\nu_e}$ [73], with $\varepsilon = \langle E^2 \rangle / \langle E \rangle$. The fact that electron antineutrinos have larger average energies than electron neutrinos suggest neutron rich ejecta. However, one has also to consider the other energy scale in the problem, i.e. the neutron to proton mass difference. It turns out that neutron-rich ejecta are only obtained when $\varepsilon_{\bar{\nu}_e} - \varepsilon_{\nu_e} > 4(m_n - m_p)$ [60, 74, 75]. As the treatment of neutrino transport and neutrino matter interactions improved over the years the energy difference between electron antineutrinos and neutrinos decreased and different simulations [76, 77, 78] obtained proton-rich ejecta during the early times of the explosion. Supernova simulations based on three-flavor Boltzmann neutrino transport have been extended to time scales of several tens of seconds [79, 80], covering the whole deleptonization of the PNS. They have predicted a continuous decrease of the energy difference between neutrinos and antineutrinos of all flavors that became practically indistinguishable after ≈ 10 s.

With the development of three-flavor Boltzmann neutrino transport codes it has been possible to relate the spectra of the emitted neutrinos and the underlying nucleosynthesis to high density neutrino matter interactions and basic properties of the nuclear equation of state. Recently, it has been shown that the energy difference between electron neutrinos and antineutrinos, and consequently the Y_e of the ejecta, is very sensitive to the treatment of charged-current reactions $\nu_e + n \rightarrow p + e^-$ and $\bar{\nu}_e + p \rightarrow n + e^+$ in neutron rich matter at densities $\rho \approx 10^{12}-10^{14}$ g cm $^{-3}$ [69, 70, 71].

Figure 2 shows the opacities or inverse mean free paths for the main processes determining the interaction of (anti)neutrinos with matter. The figure shows also the position of the energy and transport neutrinospheres for the different neutrino flavors (see ref. [81] for a description of the different processes and the determination of the neutrinospheres). One clearly sees the hierarchy mentioned above with $\nu_{\mu,\tau}$ (anti)neutrinos decoupling at the highest densities, $\bar{\nu}_e$ at intermediate densities and ν_e at the lowest densities. For the conditions considered in the figure (around 1 s postbounce) the neutrinospheres are located in the density range $10^{12}-10^{13}$ g cm $^{-3}$, i.e. $10^{-3}-10^{-2} \rho_0$ with ρ_0 the nuclear saturation density. Only for times around 10 s or later do the neutrinospheres move at densities around the saturation density.

Neutrinos are in thermal equilibrium with matter for densities larger than the location of the energy sphere, at lower densities neutrinos have decoupled from matter but still suffer several scattering events with nucleons till they reach the transport neutrinosphere [82]. The region between the energy and transport spheres constitutes a scattering atmosphere where due to the slightly inelastic nature of neutrino-nucleon scattering the spectra of neutrinos is modified [82]. This aspect is important for the determination of the $\bar{\nu}_e$ and $\nu_{\mu,\tau}$ spectra (see figure 2).

The thermal equilibrium of neutrinos with matter is maintained by processes in which the neutrino exchanges energy. As can be seen from 2, the most important processes are charged-current $\nu_e + n \rightarrow p + e^-$ and $\bar{\nu}_e + p \rightarrow n + e^+$. For the process $\nu_e + n \rightarrow p + e^-$, the opacity or inverse mean free path of a neutrino of energy E_ν is

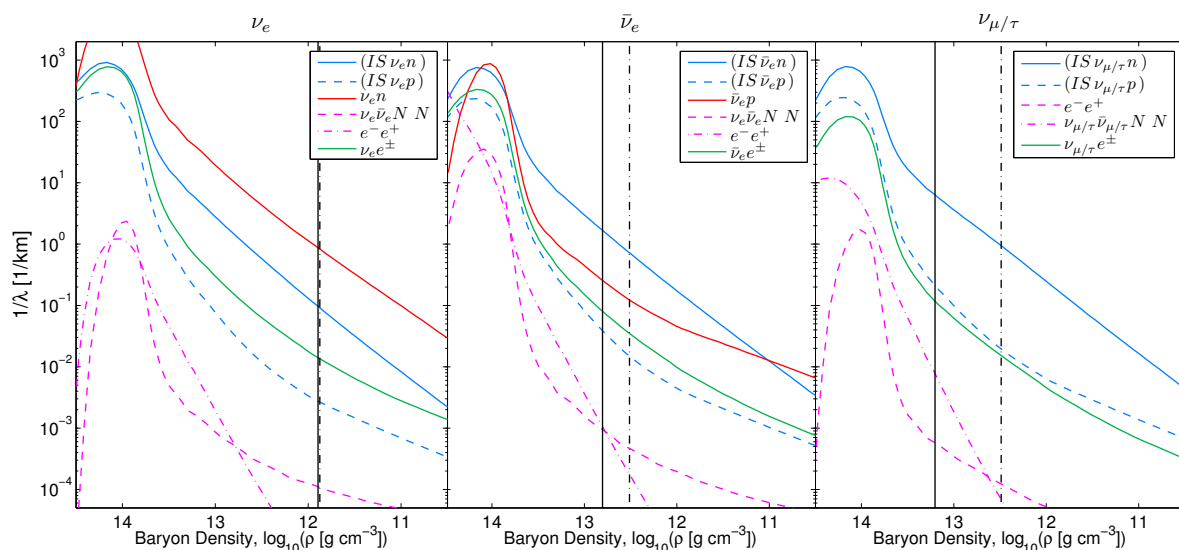


Figure 2. Inverse mean free paths for the main reactions contributing to the determination of the spectra of neutrinos emitted from a protoneutron star: isoenergetic neutrino-nucleon scattering (IS, νN), charged-current reactions ($\nu_e n$, $\bar{\nu}_e p$), N - N -Bremsstrahlung ($\nu\bar{\nu}NN$), e^-e^+ annihilation, and neutrino electron/positron scattering (νe^\pm). The different panels show the inverse mean free path for ν_e (left), $\bar{\nu}_e$ (middle) and $\nu_{\mu,\tau}$ (right) based on radial profiles at 1 second post bounce for the 18.0 M_\odot progenitor simulations of ref [80]. The vertical black solid and dash-dotted lines mark the position of the energy and transport neutrinospheres. Figure adapted from ref. [81].

given by [83, 71]:

$$\chi(E_\nu) = \frac{G_F^2 V_{ud}^2}{(\hbar c)^7} (g_V^2 + 3g_A^2) \int \frac{d^3 p_e}{(2\pi)^3} [1 - f_e(E_e)] S(q_0, q) \quad (1)$$

where f is the Fermi-Dirac distribution function and $S(q_0, q)$ is the response function of the nuclear medium that is assumed identical for Fermi and Gamow-Teller operators. The energy transfer to the medium is $q_0 = E_\nu - E_e$ and the magnitude of the momentum transfer is $q = |\mathbf{p}_\nu - \mathbf{p}_e|$. Equations of State commonly used in core-collapse supernova simulations (see, e.g., refs [84, 85]) treat neutrons and protons as a gas of non-interacting quasiparticles that move in a mean-field single-particle potential, U . In relativistic mean-field models the energy-momentum dispersion relation becomes:

$$E_i(p) = \sqrt{p^2 + m_i^{*2}} + U_i, \quad (2)$$

where m_i^* is the nucleon effective mass. For the neutron-rich conditions around the neutrinospheres the mean-field potential for neutrons and protons can be very different with their relative difference $\Delta U = U_n - U_p$ directly related to the nuclear symmetry energy [83, 86]. Ref. [83] provides analytic expressions for the response function valid both in the relativistic and non-relativistic limits that can be used for the calculation of the opacity. A simplified expression can be obtained assuming that zero momentum transfer, $q \approx 0$, reflecting the fact that nucleons are more massive than leptons. In this

case, the energy transfer becomes $q_0 = -(m_n^* - m_p^*) - \Delta U = -\Delta m^* - \Delta U$ and the opacity is given by (elastic approximation) [83, 87]:

$$\chi(E_\nu) = \frac{G_F^2 V_{ud}^2}{\pi(\hbar c)^4} (g_V^2 + 3g_A^2) p_e E_e [1 - f_e(E_e)] \frac{n_n - n_p}{1 - e^{(\varphi_p - \varphi_n)/T}}, \quad (3)$$

with $\varphi_i = \mu_i - m_i^* - U_i$, μ_i the chemical potential of the nucleon and $E_e = E_\nu + \Delta m^* + \Delta U$. If we consider neutrinos with energies smaller than $E_\nu^0 = \mu_e - \Delta m^* - \Delta U$, that varies between 10 and 30 MeV when the density varies in the range 10^{12} – 10^{13} g cm $^{-3}$, the opacity behaves as:

$$\chi(E_\nu) \propto (E_\nu + \Delta m^* + \Delta U)^2 \exp\left(\frac{E_\nu + \Delta m^* + \Delta U - \mu_e}{T}\right). \quad (4)$$

The opacity increases by an exponential factor due to the inclusion of mean-field modifications, ΔU , to the vacuum Q-value, Δm^* . Due to the strong sensitivity of the opacity to the neutrino energy, the density at which neutrinos decouple increases with decreasing neutrino energy. However, ΔU increases with density implying that the smaller is the energy of the neutrino emitted from the protoneutron star the larger the opacity correction due to the inclusion of mean-field effects (see figure 6 of ref. [71]). As the opacity for neutrinos mainly determines the deleptonization rate, i.e. the neutrino luminosity of the protoneutron star, we expect that the larger the ΔU correction, i.e. the larger the symmetry energy, the smaller the neutrino luminosity. This is in fact confirmed by Boltzmann transport simulations [69, 88].

For $\bar{\nu}_e$ there is no final state blocking for the produced positron and consequently the main effect of mean-field corrections is to change the energy threshold for neutrino absorption. Using a similar analysis than the above it can be shown that the opacity for antineutrinos behaves like:

$$\chi(E_{\bar{\nu}_e}) \propto (E_{\bar{\nu}_e} - \Delta m^* - \Delta U)^2. \quad (5)$$

The discussion above shows that mean-field effects increase the opacity for neutrino absorption while reducing the opacity for antineutrino absorption. When compared with simulations that do not include mean-field effects the increase of opacity for neutrinos will keep them in thermal equilibrium with matter up to larger radii. They decouple in regions of lower temperature and consequently their average energy is smaller. The average energy of antineutrinos is expected to increase as they decouple at slightly deeper (hotter) regions of the neutron star. However, due to the reduced dominance of charged-current reactions (see figure 2) the change in average energy is expected to be smaller for $\bar{\nu}_e$. This has been confirmed by recent long term simulations of PNS cooling [69, 70, 71] that treat charged-current opacities consistently with the EoS at the mean-field level. They have shown that the inclusion of mean-field effects increases the energy difference between $\bar{\nu}_e$ and ν_e with respect to the values obtained without mean-field effects. For the nucleosynthesis point view, the main consequence is that ejecta that were proton-rich during the whole deleptonization period of the protoneutron star now become neutron-rich during the first seconds and later turn proton-rich as the energy

difference between $\bar{\nu}_e$ and ν_e decreases. The neutron-richness of the ejecta depends on the symmetry energy of the underlying EoS. Hence, it becomes important to use an EoS that reproduce recent constraints on the symmetry energy.

Notice that the symmetry energy does not only affect the evolution during the deleptonization phase but determines the whole structure of the protoneutron star after the onset of the explosion. Electron captures on nuclei determine the amount of deleptonization occurring during the collapse [89]. At the onset of neutrino trapping, at densities around 10^{12} g cm $^{-3}$, Y_e reaches a value $Y_e^{\text{trap}} \approx 0.3$ [90]. At this moment electron (anti)neutrinos thermalize and the system reaches weak equilibrium, $\mu_{\nu_e} + \mu_n = \mu_e + \mu_p$. Once the core reaches nuclear matter densities and a transition to uniform nuclear matter occurs the relative ratio of neutrons and protons (and electrons and neutrinos) is fully determined by the symmetry energy under the constrain of constant lepton number, $Y_{\text{lep}} = Y_e + Y_{\nu_e} = Y_e^{\text{trap}}$. This can be seen from the following relation [86]:

$$\mu_e - \mu_{\nu_e} = \mu_n - \mu_p = 4(1 - 2Y_e)S(\rho), \quad (6)$$

with $S(\rho)$ the nuclear symmetry energy. As protons and neutrinos have rather low abundances, their exact value is rather sensitive to changes of the symmetry energy. This implies that in order to determine the impact of a particular EoS on the nucleosynthesis outcome of neutrino-driven winds it is important to cover all relevant supernova phases including core-collapse, bounce, post-bounce accretion, explosion and cooling. In particular, the high Y_e values obtained at early times ($\lesssim 1$ s) in the protoneutron star evolution simulations of ref. [70] could be an artifact of the particular progenitor used. This caveat was noted in ref. [70] but was not accounted for in the nucleosynthesis study of ref. [72]. Due to their large mass loss rate [72], the early cooling phase is particularly important for determining the mass-integrated nucleosynthesis of neutrino-driven winds. To accurately resolve the transition between accretion and cooling phases requires multidimensional simulations [91].

The equation of state for neutron-matter has been recently computed using all many-body forces among neutrons predicted by chiral effective field theory (EFT) up to next-to-next-to-next-to-leading order (N³LO) [92, 93]. The predicted energy per nucleon for neutron-matter is shown in the left panel of figure 3. When compared with equations of state used in core-collapse simulations (see figure 9 of ref. [93]) one finds that the two most commonly used, the non-relativistic Skyrme-like of Lattimer and Swesty [84] and the relativistic mean-field (RMF) based on the TM1 functional [85], are not consistent with chiral EFT constraints particularly at subsaturation densities. An EoS that reproduces these constraints is the RMF based on the density-dependent DD2 functional [95] (see figure 3). In addition, the DD2 based EoS reproduces constraints on the symmetry energy at saturation density from chiral EFT [93] and a global analysis combining nuclear experimental information and astronomical observations of neutron stars [94]. The symmetry energy predicted by the DD2 EoS is shown in the right panel of fig. 3 for the whole range of densities relevant for neutrino-wind simulations. Notice that

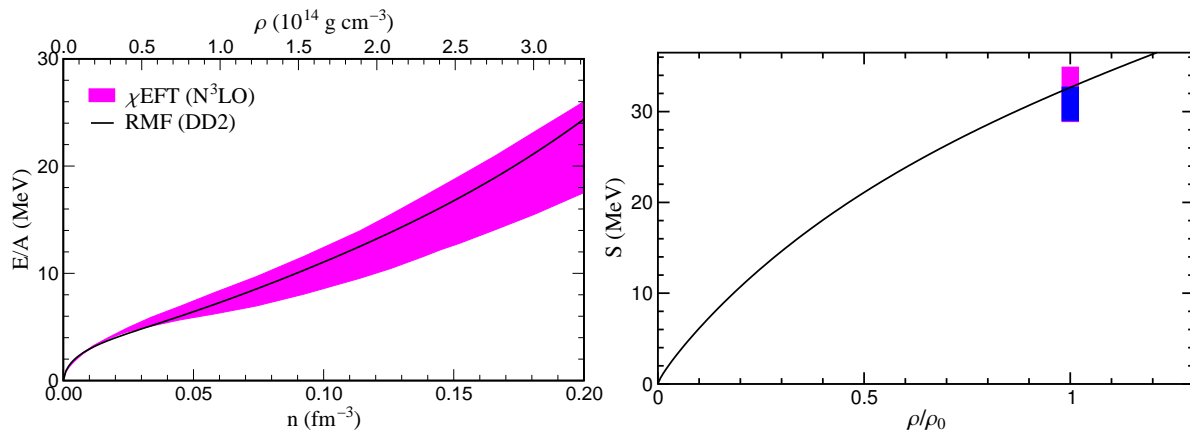


Figure 3. (left panel) Energy per nucleon for neutron matter computed by chiral EFT interactions computed up to $N^3\text{LO}$ order [92, 93]. The magenta band includes uncertainty estimates due to the many-body calculation, low-energy constants and the regularization cutoffs in the 3N and 4N forces (see ref. [93] for additional details). The black line shows the energy per nucleon predicted by RMF calculations using the density dependent DD2 functional. (right panel) Symmetry energy, defined as the difference between the energy per nucleon for neutron and symmetric matter, determined by the RMF DD2 calculations compared with recent constrains from chiral EFT [93] (magenta box) and nuclear physics experiments and astronomical observations [94] (blue box).

clustering effects that are expected to be important at subsaturation densities [96] are not included in the calculation of the symmetry energy. The DD2 EoS also reproduces constraints on the maximum mass of neutron stars and comes close (within 1 km) to the recent estimates of the observational radius [97].

4. Nucleosynthesis in neutrino-driven winds

We have performed core-collapse supernova simulations based on spherically symmetric radiation hydrodynamics with three-flavor Boltzmann neutrino transport using the AGILE-Boltztran code. In the high density regime, we use the DD2 EoS table provided by M. Hempel§. The equation of state is based on the extended nuclear statistical model of ref. [98] and includes a detailed nuclear composition allowing for the presence of light nuclear clusters at subsaturation densities. Importantly, the EoS provides the mean-field corrections necessary for the calculation of charged-current neutrino reactions. Additional details will be provided in a forthcoming publication. The simulations are based on the $11.2 M_{\odot}$ progenitor of ref. [99]. Because spherically symmetric simulations do not result in explosions for this iron-core progenitor, we enhance the neutrino heating rates in the gain region following the scheme of ref. [80]. The simulations are evolved from core collapse, through the explosion up to 9 seconds after bounce. Figure 4 shows the evolution of the luminosities and average energies for all neutrino flavors (left panels).

§ <http://phys-merger.physik.unibas.ch/~hempel/eos.html>

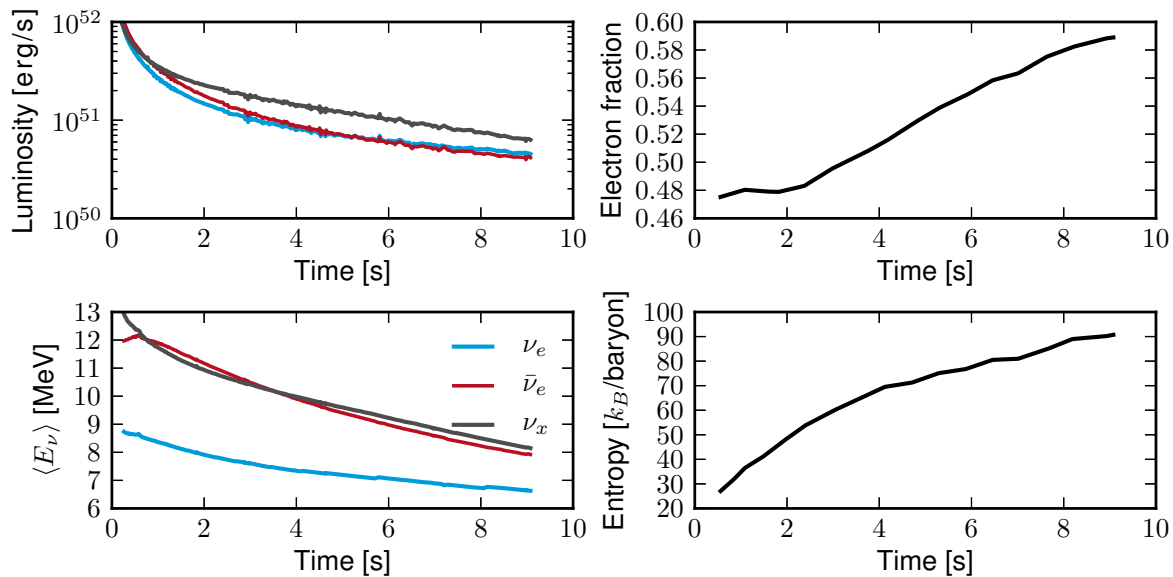


Figure 4. The left panels show the evolution of neutrino luminosities (upper) and average neutrino energies (lower) for the different neutrino flavors. The right panels show the asymptotic values of entropy (lower) and Y_e (upper) reached in the ejecta.

The right panels show the evolution of the values of Y_e and entropy asymptotically reached by the ejecta. One sees that the early ejecta is neutron rich with $Y_e \sim 0.48$. This value is larger than the one previously found in ref. [69] using the TM1 EoS [85]. The Y_e values have been determined using a full nuclear network that includes neutrino interactions both on nucleons and nuclei and accounts for the so-called α -effect [100].

The mass-integrated nucleosynthesis is shown in figure 5. The upper panel shows the mass-integrated isotopic abundances normalized to the solar abundances. The lower panel shows the mass-integrated elemental abundances compared with the observations of the metal-poor star enriched in light r-process elements HD 122563 [30]. The stellar observations have been arbitrarily normalized to Zn ($Z = 30$). Our calculations reproduce the observed abundance of Zr ($Z = 40$) and other nuclei around $A = 90$ within a factor 4. The production of these $N = 50$ closed neutron shell nuclei is rather sensitive to Y_e . They will be overproduced if $Y_e \lesssim 0.47$ [101]. Our results indicate that neutrino-driven winds are the site for the production of elements like Sr, Y and Zr. This is in agreement with the correlation observed in figure 1 as core-collapse supernova are the main contributors for Fe at low metallicities [102]. In our calculations, the elements Sr, Y, Zr, Nb, and Mo are produced mainly in the early neutron-rich ejecta by charged-particle reactions together with some neutron captures. Due to the sudden drop of alpha and neutron separation energies around $N = 50$ the production of nuclei with $N > 50$ decreases dramatically (see upper panel figure 5). Nuclei with $Z > 42$ ($A > 92$) are mainly produced in the late proton-rich ejecta by the νp -process [103, 104, 105]. However their production is very inefficient due to the low antineutrino luminosities at late times. The production of elements with $A > 64$ by the νp -process is very sensitive

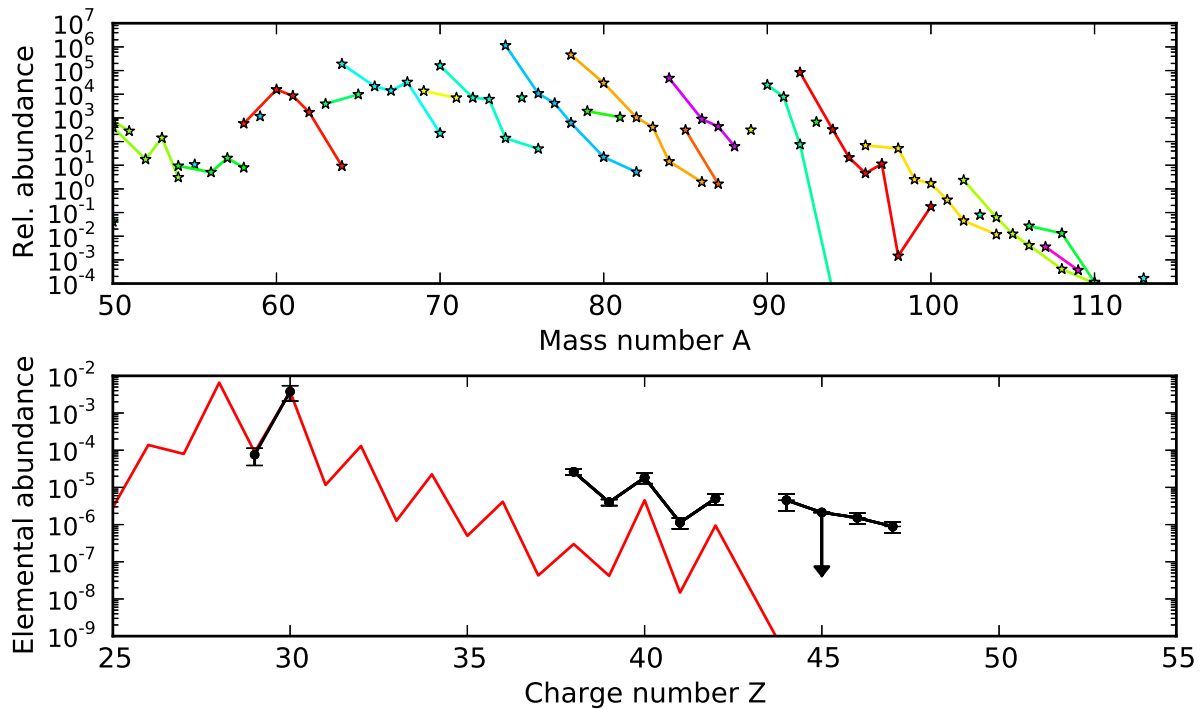


Figure 5. Mass-integrated neutrino wind abundances. The upper panel shows the ratio between the abundance of a nucleus normalized to the solar abundance. The lower panel shows the elemental abundances (red) compared with the observations of HD 122563 [30] (black).

to the rate of antineutrino absorption on protons [106] that is directly proportional to the luminosity. Our value is around an order of magnitude smaller than those used in refs. [68, 72] but consistent with recent Boltzmann transport simulations [79, 70]. In addition, the amount of material ejected at later times is very small to contribute significantly to the mass-integrated abundances.

If our results represent an standard situation for neutrino-driven winds, the obvious question then is: where are the elements with $Z > 42$ (including Ag and Pd) produced? A recent study [39] has shown that the evolution with metallicity of Ag and Pd is uncorrelated with both $N = 50$ elements (Sr, Y and Zr) and heavy r-process elements (Eu and Ba). Despite of being consistent with our results, it represents a challenge for nucleosynthesis models as it is very difficult to find astrophysical conditions where Ag and Pd are produced without synthesizing neither $N = 50$ elements nor heavy r-process elements. This also applies to electron-capture supernova that have been suggested as a possible site for the production of elements between Ge and Zr [107]. Another open problem that cannot be explained by our simulations is the correlation between Eu and Fe observed in figure 1.

Due to the relatively large values of Y_e achieved in our nucleosynthesis calculations, only the neutron-deficient isotopes of elements between Ge and Mo are produced. This can be tested by observations of isotopic abundances in metal-poor stars. At the same

time it requires that the neutron-rich isotopes, that normally cannot be produced by the s-process [27], are produced in some other astrophysical site. Due to the more neutron-rich conditions achieved in electron-capture supernova [107] it is expected that their distribution will be richer in neutron-rich isotopes. An alternative site (but probably more speculative) is core-collapse supernova explosions due to a quark-hadron phase transition [108]. It is interesting to notice that ^{92}Mo , a nucleus that is difficult to produce by the p-process [16], is abundantly produced in our calculations.

5. Summary

We have analyzed recent evidence of metal-poor stars that show the existence of two distinctive sources for the production of r-process nuclei with different frequencies along Galactic history [34]. There is strong evidence that core-collapse supernova could be the site for the production of light r-process elements including Sr, Y and Zr (sometimes also denoted as LEPP elements) [68]. They will account for the abundances of elements observed in metal-poor stars that are enriched in light r-process elements but depleted in heavy r-process elements. HD 122563 [30, 31] constitutes the classical example. Looking at the evolution with metallicity of several light r-process elements and Eu, that is taken as a representative of heavy r-process elements, in HD 122563 type stars we find a strong correlation. It indicates that in fact the abundances of Sr, Y and Zr seen in these stars are due to core-collapse supernova that is the major producer of iron at low metallicity. The situation for Ag is unclear as only two of the stars that survive our selection criteria have observed abundances of Ag. A recent study has in fact shown that the abundance of Ag is anticorrelated with Sr, Y and Zr [39]. Surprisingly, we also find that the Eu abundance observed on HD 122563 type stars is correlated with Fe. It will be interesting to see if this correlation extends to other elements like Ba.

We have presented first long-term Boltzmann transport neutrino-wind simulations based on a core-collapse supernova equation of state that reproduces recent constraints on the nuclear symmetry energy at saturation densities [94, 93] and on the energy per nucleon of neutron matter [93]. Our simulations consistently include mean-field corrections for neutrons and protons [83, 69, 71] for the (anti)neutrino opacities at high density. These corrections increase substantially the opacity for ν_e . The increase being largest the larger the mean-field energy difference between neutrons and protons, i.e. the larger the symmetry energy of the EoS. A larger symmetry energy implies a larger difference between the average energies of the emitted $\bar{\nu}_e$ and ν_e [69, 71, 109] and a smaller neutrino luminosity [88, 69]. Both aspects are important for determining the nucleosynthesis in neutrino-driven winds.

Our simulations predict that the early neutrino-driven wind ejecta is neutron-rich with $Y_e \approx 0.48$. At times around 4 s the ejecta become proton-rich reaching $Y_e = 0.586$ at 9 s when our simulation stops. We have analyzed the nucleosynthesis outcome of the simulations. Our results show that neutrino-driven winds do not produce heavy r-process elements. They contribute to the production of elements between Zn and Mo, including

^{92}Mo that is largely underproduced by the p-process in massive stars [16]. The elemental abundances are consistent with the observations of the metal-poor star HD 12263. For elements between Ge and Mo, we produce mainly the neutron-deficient isotopes. This prediction could be confirmed by observations of isotopic abundances in metal-poor stars. No elements heavier than Mo ($Z = 42$) are produced in our calculations. In neutron-rich ejecta, their production is suppressed due to the $N = 50$ shell closure. In the late proton-rich ejecta, the νp -process, that in principle can contribute to their production, is very inefficient due to the low antineutrino luminosities.

Even if our nucleosynthesis study is based on parameter free Boltzmann transport simulations, there are still some sources of uncertainty on the determination of the (anti)neutrino opacities. One is the treatment of neutrino interactions with light nuclear clusters, in particular ^2H , ^3H . They are expected to be present in the region of neutrino decoupling [110] and in fact the equation of state we use predicts them with large abundances (see figure 10 of ref. [97]). The presence of light nuclear clusters affects the (anti)neutrino opacities in different ways. First, it modifies the mean-field corrections for the unbound nucleons [109]. This effect is included in our simulations. Secondly, it becomes necessary to consider both charged and neutral current interactions with the light clusters. The relevant cross sections have been computed for the deuteron [111, 112, 113] and triton [110] in vacuum. However, their presence in the nuclear medium will induce changes in the energy thresholds for the reactions due to different in medium modifications for the for the initial and final states. Furthermore, the wave functions [114] for the cluster will be modified with respect to the vacuum case affecting the response to (anti)neutrinos.

An accurate determination of the (anti)neutrino spectra and luminosities and their evolution with time is also necessary for neutrino flavor oscillations in supernova [10, 9] and neutrino detection on Earth. From the point of view of nucleosynthesis in neutrino-driven winds collective neutrino oscillations [10] are most relevant. It remains to evaluate the impact that they may have on the nucleosynthesis. Another important effect is the possibility of oscillations of active to sterile neutrinos, suggested to explain the reactor anomaly [115]. Oscillations to the sterile flavor can affect both the dynamics during the supernova explosion [116, 117] and the neutrino-driven wind nucleosynthesis [118, 117].

Acknowledgments

G.M.P. and L.H. is partly supported by the Deutsche Forschungsgemeinschaft through contract SFB 634, the Helmholtz International Center for FAIR within the framework of the LOEWE program launched by the state of Hesse, and the Helmholtz Association through the Nuclear Astrophysics Virtual Institute (VH-VI-417). T.F. acknowledges support from the Narodowe Centrum Nauki (NCN) within the ‘‘Maestro’’ program under contract No. DEC- 2011/02/A/ST2/00306. We gratefully acknowledge Stefan Typel and Thomas Krüger for providing the data for figure 3. The supernova simulations were performed at the computer cluster at the GSI Helmholtzzentrum for

Schwerionenforschung GmbH, Darmstadt (Germany).

References

- [1] Bethe H A 1990 *Rev. Mod. Phys.* **62** 801
- [2] Janka H T, Langanke K, Marek A, Martínez-Pinedo G and Müller B 2007 *Phys. Repts.* **442** 38
- [3] Bethe H A and Wilson J R 1985 *Astrophys. J.* **295** 14
- [4] Müller B, Janka H T and Marek A 2012 *Astrophys. J.* **756** 84
- [5] Bruenn S W, Mezzacappa A, Hix W R, Lentz E J, Bronson Messer O E, Lingerfelt E J, Blondin J M, Endeve E, Marronetti P and Yakunin K N 2013 *Astrophys. J.* **767** L6
- [6] Suwa Y, Takiwaki T, Kotake K, Fischer T, Liebendörfer M and Sato K 2013 *Astrophys. J.* **764** 99
- [7] Duncan R C, Shapiro S L and Wasserman I 1986 *Astrophys. J.* **309** 141
- [8] Arcones A and Thielemann F K 2013 *J. Phys. G: Nucl. Part. Phys.* **40** 013201
- [9] Duan H and Kneller J P 2009 *J. Phys. G: Nucl. Part. Phys.* **36** 113201
- [10] Duan H, Fuller G M and Qian Y 2010 *Ann. Rev. Nucl. Part. Sci.* **60** 569
- [11] Woosley S E, Hartmann D H, Hoffman R D and Haxton W C 1990 *Astrophys. J.* **356** 272
- [12] Heger A, Kolbe E, Haxton W, Langanke K, Martínez-Pinedo G and Woosley S E 2005 *Phys. Lett. B* **606** 258
- [13] Banerjee P, Haxton W C and Qian Y Z 2011 *Phys. Rev. Lett.* **106** 201104
- [14] Burbidge E M, Burbidge G R, Fowler W A and Hoyle F 1957 *Rev. Mod. Phys.* **29** 547
- [15] Cameron A G W 1957 Stellar evolution, nuclear astrophysics, and nucleogenesis Report CRL-41 Chalk River
- [16] Arnould M and Goriely S 2003 *Phys. Repts.* **384** 1
- [17] Straniero O, Gallino R and Cristallo S 2006 *Nucl. Phys. A* **777** 311
- [18] Busso M, Gallino R and Wasserburg G J 1999 *Annu. Rev. Astron. Astrophys.* **37** 239
- [19] Pignatari M, Gallino R, Heil M, Wiescher M, Käppeler F, Herwig F and Bisterzo S 2010 *Astrophys. J.* **710** 1557
- [20] Arnould M, Goriely S and Takahashi K 2007 *Phys. Repts.* **450** 97
- [21] Lodders K 2003 *Astrophys. J.* **591** 1220
- [22] Asplund M, Grevesse N, Sauval A J and Scott P 2009 *Ann. Rev. Astron. Astrophys.* **47** 481
- [23] Jacobson H R and Frebel A 2013 [arXiv:1309.0037](https://arxiv.org/abs/1309.0037) [astro-ph.GA]
- [24] Arlandini C, Käppeler F, Wisshak K, Gallino R, Lugaro M, Busso M and Straniero O 1999 *Astrophys. J.* **525** 886
- [25] Bisterzo S, Gallino R, Straniero O, Cristallo S and Käppeler F 2010 *Mon. Not. Roy. Ast. Soc.* **404** 1529
- [26] Cowan J J and Sneden C 2006 *Nature* **440** 1151
- [27] Sneden C, Cowan J J and Gallino R 2008 *Ann. Rev. Astron. Astrophys.* **46** 241
- [28] Christlieb N *et al.* 2004 *Astron. & Astrophys.* **428** 1027
- [29] Roederer I U and Lawler J E 2012 *Astrophys. J.* **750** 76
- [30] Honda S, Aoki W, Ishimaru Y, Wanajo S and Ryan S G 2006 *Astrophys. J.* **643** 1180
- [31] Roederer I U, Lawler J E, Sobeck J S, Beers T C, Cowan J J, Frebel A, Ivans I I, Schatz H, Sneden C and Thompson I B 2012 *Astrophys. J. Suppl.* **203** 27
- [32] Woosley S E and Hoffman R D 1992 *Astrophys. J.* **395** 202
- [33] Witt J, Janka H T and Takahashi K 1994 *Astron. & Astrophys.* **286** 841
- [34] Qian Y Z and Wasserburg G J 2007 *Phys. Repts.* **442** 237
- [35] Travaglio C, Gallino R, Arnone E, Cowan J, Jordan F and Sneden C 2004 *Astrophys. J.* **601** 864
- [36] Burris D L, Pilachowski C A, Armandroff T E, Sneden C, Cowan J J and Roe H 2000 *Astrophys. J.* **544** 302
- [37] Honda S, Aoki W, Kajino T, Ando H, Beers T C, Izumiura H, Sadakane K and Takada-Hidai M 2004 *Astrophys. J.* **607** 474

- [38] Barklem P S, Christlieb N, Beers T C, Hill V, Bessell M S, Holmberg J, Marsteller B, Rossi S, Zickgraf F J and Reimers D 2005 *Astron. & Astrophys.* **439** 129
- [39] Hansen C J, Primas F, Hartman H, Kratz K L, Wanajo S, Leibundgut B, Farouqi K, Hallmann O, Christlieb N and Nilsson H 2012 *Astron. & Astrophys.* **545** A31
- [40] Cowan J J and Thielemann F K 2004 *Physics Today* **57** 47
- [41] Wasserburg G J and Qian Y Z 2000 *Astrophys. J.* **529** L21
- [42] Roederer I U 2013 *Astron. J.* **145** 26
- [43] Montes F *et al.* 2007 *Astrophys. J.* **671** 1685
- [44] Korobkin O, Rosswog S, Arcones A and Winteler C 2012 *Mon. Not. Roy. Ast. Soc.* **426** 1940
- [45] Bauswein A, Goriely S and Janka H T 2013 *Astrophys. J.* **773** 78
- [46] Martínez-Pinedo G 2008 *J. Phys. G: Nucl. Part. Phys.* **35** 014057
- [47] Petermann I, Langanke K, Martínez-Pinedo G, Panov I V, Reinhard P G and Thielemann F K 2012 *Eur. Phys. J. A* **48** 122
- [48] Metzger B D, Martínez-Pinedo G, Darbha S, Quataert E, Arcones A, Kasen D, Thomas R, Nugent P, Panov I V and Zinner N T 2010 *Mon. Not. Roy. Ast. Soc.* **406** 2650
- [49] Roberts L F, Kasen D, Lee W H and Ramirez-Ruiz E 2011 *Astrophys. J.* **736** L21
- [50] Tanvir N R, Levan A J, Fruchter A S, Hjorth J, Hounsell R A, Wiersema K and Tunnicliffe R L 2013 *Nature* **500** 547
- [51] Berger E, Fong W and Chornock R 2013 *Astrophys. J.* **774** L23
- [52] Grossman D, Korobkin O, Rosswog S and Piran T 2013 arXiv:1307.2943 [astro-ph.HE]
- [53] Wanajo S and Janka H T 2012 *Astrophys. J.* **746** 180
- [54] Fernández R and Metzger B D 2013 *Mon. Not. Roy. Ast. Soc.* arXiv:1304.6720 [astro-ph.HE]
<http://dx.doi.org/10.1093/mnras/stt1312>
- [55] Qian Y Z 2000 *Astrophys. J.* **534** L67
- [56] Argast D, Samland M, Thielemann F K and Qian Y Z 2004 *Astron. & Astrophys.* **416** 997
- [57] Winteler C, Käppeli R, Perego A, Arcones A, Vasset N, Nishimura N, Liebendörfer M and Thielemann F K 2012 *Astrophys. J.* **750** L22
- [58] Woosley S E, Wilson J R, Mathews G J, Hoffman R D and Meyer B S 1994 *Astrophys. J.* **433** 229
- [59] Takahashi K, Wittl J and Janka H T 1994 *Astron. & Astrophys.* **286** 857
- [60] Qian Y Z and Woosley S E 1996 *Astrophys. J.* **471** 331
- [61] Hoffman R D, Woosley S E and Qian Y Z 1997 *Astrophys. J.* **482** 951
- [62] Otsuki K, Tagoshi H, Kajino T and Wanajo S 2000 *Astrophys. J.* **533** 424
- [63] Thompson T A, Burrows A and Meyer B S 2001 *Astrophys. J.* **562** 887
- [64] Arcones A, Janka H T and Scheck L 2007 *Astron. & Astrophys.* **467** 1227
- [65] Arcones A and Janka H T 2011 *Astron. & Astrophys.* **526** A160
- [66] Kuroda T, Wanajo S and Nomoto K 2008 *Astrophys. J.* **672** 1068
- [67] Roberts L F, Woosley S E and Hoffman R D 2010 *Astrophys. J.* **722** 954
- [68] Arcones A and Montes F 2011 *Astrophys. J.* **731** 5
- [69] Martínez-Pinedo G, Fischer T, Lohs A and Huther L 2012 *Phys. Rev. Lett.* **109** 251104
- [70] Roberts L F 2012 *Astrophys. J.* **755** 126
- [71] Roberts L F, Reddy S and Shen G 2012 *Phys. Rev. C* **86** 065803
- [72] Wanajo S 2013 *Astrophys. J.* **770** L22
- [73] Keil M T, Raffelt G G and Janka H T 2003 *Astrophys. J.* **590** 971
- [74] Fröhlich C *et al.* 2006 *Astrophys. J.* **637** 415
- [75] Martínez-Pinedo G 2008 *Eur. Phys. J. Special Topics* **156** 123
- [76] Buras R, Rampp M, Janka H T and Kifonidis K 2006 *Astron. & Astrophys.* **447** 1049
- [77] Liebendörfer M, Mezzacappa A, Thielemann F K, Bronson Messer O E, Raphael Hix W and Bruenn S W 2001 *Phys. Rev. D* **63** 103004
- [78] Thompson T A, Quataert E and Burrows A 2005 *Astrophys. J.* **620** 861
- [79] Hüdepohl L, Müller B, Janka H, Marek A and Raffelt G G 2010 *Phys. Rev. Lett.* **104** 251101

- [80] Fischer T, Whitehouse S C, Mezzacappa A, Thielemann F K and Liebendörfer M 2010 *Astron. & Astrophys.* **517** A80
- [81] Fischer T, Martínez-Pinedo G, Hempel M and Liebendörfer M 2012 *Phys. Rev. D* **85** 083003
- [82] Raffelt G G 2001 *Astrophys. J.* **561** 890
- [83] Reddy S, Prakash M and Lattimer J M 1998 *Phys. Rev. D* **58** 013009
- [84] Lattimer J M and Swesty F D 1991 *Nucl. Phys. A* **535** 331
- [85] Shen H, Toki H, Oyamatsu K and Sumiyoshi K 1998 *Nucl. Phys. A* **637** 435
- [86] Haensel P, Potekhin A Y and Yakovlev D G 2007 *Neutron Stars 1: Equation of State and Structure* volume 326 of *Astrophysics and Space Science Library* (Springer, New York)
- [87] Bruenn S W 1985 *Astrophys. J. Suppl.* **58** 771
- [88] Roberts L F, Shen G, Cirigliano V, Pons J A, Reddy S and Woosley S E 2012 *Phys. Rev. Lett.* **108** 061103
- [89] Langanke K and Martínez-Pinedo G 2003 *Rev. Mod. Phys.* **75** 819
- [90] Martínez-Pinedo G, Liebendörfer M and Frekers D 2006 *Nucl. Phys. A* **777** 395
- [91] Müller B, Janka H T and Heger A 2012 *Astrophys. J.* **761** 72
- [92] Tews I, Krüger T, Hebeler K and Schwenk A 2013 *Phys. Rev. Lett.* **110** 032504
- [93] Krüger T, Tews I, Hebeler K and Schwenk A 2013 *Phys. Rev. C* **88** 025802
- [94] Lattimer J M and Lim Y 2013 *Astrophys. J.* **771** 51
- [95] Typel S, Röpke G, Klähn T, Blaschke D and Wolter H H 2010 *Phys. Rev. C* **81** 015803
- [96] Horowitz C J and Schwenk A 2006 *Nucl. Phys. A* **776** 55
- [97] Fischer T, Hempel M, Sagert I, Suwa Y and Schaffner-Bielich J 2013 [arXiv:1307.6190](https://arxiv.org/abs/1307.6190) [astro-ph.HE]
- [98] Hempel M and Schaffner-Bielich J 2010 *Nucl. Phys. A* **837** 210
- [99] Woosley S E, Heger A and Weaver T A 2002 *Rev. Mod. Phys.* **74** 1015
- [100] Meyer B S, McLaughlin G C and Fuller G M 1998 *Phys. Rev. C* **58** 3696
- [101] Hoffman R D, Woosley S E, Fuller G M and Meyer B S 1996 *Astrophys. J.* **460** 478
- [102] Timmes F X, Woosley S E and Weaver T A 1995 *Astrophys. J. Suppl.* **98** 617
- [103] Fröhlich C, Martínez-Pinedo G, Liebendörfer M, Thielemann F K, Bravo E, Hix W R, Langanke K and Zinner N T 2006 *Phys. Rev. Lett.* **96** 142502
- [104] Pruet J, Hoffman R D, Woosley S E, Janka H T and Buras R 2006 *Astrophys. J.* **644** 1028
- [105] Wanaajo S 2006 *Astrophys. J.* **647** 1323
- [106] Martínez-Pinedo G, Ziebarth B, Fischer T and Langanke K 2011 *Eur. Phys. J. A* **47** 1
- [107] Wanaajo S, Janka H T and Müller B 2011 *Astrophys. J.* **726** L15
- [108] Nishimura N, Fischer T, Thielemann F K, Fröhlich C, Hempel M, Käppeli R, Martínez-Pinedo G, Rauscher T, Sagert I and Winteler C 2012 *Astrophys. J.* **758** 9
- [109] Horowitz C J, Shen G, O'Connor E and Ott C D 2012 *Phys. Rev. C* **86** 065806
- [110] Arcones A, Martínez-Pinedo G, O'Connor E, Schwenk A, Janka H, Horowitz C J and Langanke K 2008 *Phys. Rev. C* **78** 015806
- [111] Nakamura S, Sato T, Gudkov V and Kubodera K 2001 *Phys. Rev. C* **63** 034617
- [112] Nakamura S, Sato T, Ando S, Park T S, Myhrer F, Gudkov V and Kubodera K 2002 *Nucl. Phys. A* **707** 561
- [113] Shen G, Marcucci L E, Carlson J, Gandolfi S and Schiavilla R 2012 *Phys. Rev. C* **86** 035503
- [114] Röpke G, Bastian N U, Blaschke D, Klähn T, Typel S and Wolter H 2013 *Nucl. Phys. A* **897** 70
- [115] Kopp J, Machado P A N, Maltoni M and Schwetz T 2013 *Journal of High Energy Physics* **5** 50 [arXiv:1303.3011](https://arxiv.org/abs/1303.3011) [hep-ph]
- [116] Nunokawa H, Peltoniemi J T, Rossi A and Valle J W F 1997 *Phys. Rev. D* **56** 1704
- [117] Wu M R, Fischer T, Martínez-Pinedo G and Qian Y Z 2013 [arXiv:1305.2382](https://arxiv.org/abs/1305.2382) [astro-ph.HE]
- [118] Tamborra I, Raffelt G G, Hüdepohl L and Janka H T 2012 *JCAP* **01** 013